A TEM and 2D-XRD Study of the Thermal Decomposition of Calcite

/ENCARNACIÓN RUIZ-AGUDO (*), CARLOS RODRÍGUEZ-NAVARRO, ANA LUQUE, ALEJANDRO RODRÍGUEZ-NAVARRO, MIGUEL ORTEGA HUERTAS

Departamento de Mineralogía y Petrología, Facultad de Ciencias, Universidad de Granada, Fuentenueva s/n 18002 Granada (España)

INTRODUCTION.

The thermal decomposition of calcium carbonate results in the formation of lime (CaO) and the release of CO_2 (Boynton 1980). Lime, which has been traditionally used for building purposes (Elert et al. 2001), is nowadays also employed in agriculture, food processing, disinfection and disease control, water treatment, flue-gas desulfuration, steelmaking, plastics and glass fabrication, and sugar refining (Boynton, 1980). The thermal decomposition of calcite also plays a role in a number of geologic processes such as high grade metamorphism, pyrometamorphism and meteorite impacting (Best, 1982; O'Keefe and Ahrens, 1989; Grapes, 2006). Despite the numerous efforts dedicated to the understanding of this apparently simple decomposition reaction, the actual atomic scale reaction mechanism responsible for the observed textural relationships between reactant and product phases is not fully understood (Beruto et al., 2004). Here we have studied the thermal decomposition of Iceland Spar single crystals in air, at T ranging from 600 up to 1150°C. It is the aim of this work to elucidate by means of transmission electron microscopy (TEM) and selected area electron diffraction (SAED) analysis, as well as texture X-ray diffraction (2D-XRD) analysis, if the transformation mechanism is a solid state topotactic reaction as has been suggested, but never convincingly proved (Beruto et al. 2004).

MATERIALS AND METHODS.

Calcite crystals (Iceland spar, from Mexico) were calcined in an air-ventilated electric furnace (Select-Horn, Selecta), cooled at room T and kept in dry N_2 atmosphere vials. An X-ray diffraction (XRD) analysis of the phase evolution with T, was performed on a Philips PW-1710 diffractometer with an automatic slit, Cu Kα radiation (λ = 1.5405 Å), 20 to 80 °2θ explored area, with steps of 0.03 °2θ and 0.03 °2θ s⁻¹ goniometer speed (static mode, 1 s counting time).
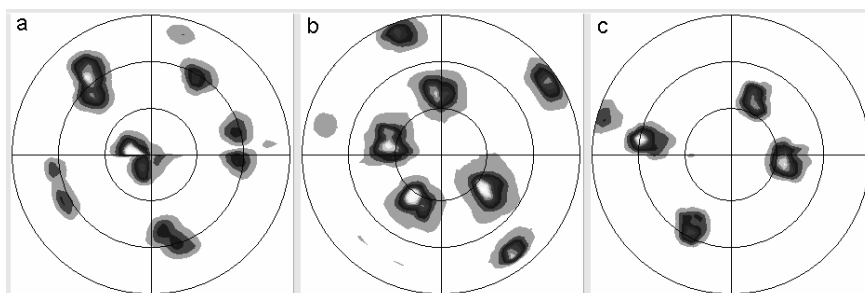
fig 1. *Pole figures of calcite pseudomorphs calcined at 850°C. Note the well defined preferred orientation of: a) (110); b) (111); and c) (100) planes. Note also the existence of two sets of crystals with (100) planes rotated ca. 80 ° with respect to each other resulting in 4 maxima in the pole figure shown in (c). Due to experimental constrains, only pole figures corresponding to planes with ρ < 85° are represented.*

The evolution of CaO crystallite size with T was calculated from peak broadening analysis using the XPowder software package (Martin-Ramos, 2004). Pole figures describing the 3-D orientation relationships between calcite pseudomorphs and product lime crystals were determined using a X-ray single crystal diffractometer equipped with an area detector (D8 SMART APEX, Bruker). The working conditions were: Mo Kα (λ = 0.7093 Å), 50 kV and 30 mA, a pin-hole collimator of 0.5 mm in diameter, and an exposure time of 20 s per frame. Iceland spar pseudomorphs were measured by reflection. A set of frames (2D diffraction patterns) was registered while rotating the sample around φ angle. Pole densities for the strongest lime reflections were calculated and displayed in stereographic projection using the XRD2DScan software (Rodriguez-Navarro, 2007). *Ex situ* TEM observations and SAED analyses of calcite pseudomorphs were performed on a Philips CM20 operated at 200 kV. *In situ* decomposition of calcite crystals (about 5 μm in size) due to electron beam damage was also observed in the TEM (i.e., high vacuum conditions).

RESULTS AND DISCUSSION.

XRD Analysis of Phase Evolution with T

The products of the thermal decomposition of calcite single crystals retained the external shape of the {10$\bar{1}$4} rhombohedron, as it has been already indicated by several researchers (Beruto et al., 2004). Partially decomposed crystals are formed by a core of unaltered carbonate, surrounded by a lime brownish shell. The reaction occurs through the formation and advance of a reactant-product interface through which the CO_2 diffuses outside (Beruto et al., 2004). The former observation suggests that there is a crystallographic control in the interface advancement towards the nucleus of the crystal.

CaO peaks were first detected in XRD patterns of powdered samples at 750°C. Calcite Bragg peaks disappeared at T > 800°C. At this point, the main CaO peaks were clearly observed. Upon further increase the temperature, CaO crystallite size increased from 27 nm (800°C) up to 76 nm (1150°C) while peak breadth decreased, which suggests that a sintering process occurred. The lime 220 reflection was the most intense in the XRD pattern of non grinded pseudomorphs (instead of 200, as in powdered samples). This suggests a preferred orientation of CaO crystals, which was further confirmed by pole figures of (111), (200) and (220) planes of CaO, obtained from 2D-XRD single-crystal analysis (Fig. 1). In particular, {110}lime planes were parallel to {10$\bar{1}$4}calcite (Fig. 1a). Curiously, pole figure of 200 lime planes showed 4 maxima instead of the 2 expected for a single crystal. This suggests that two set of CaO crystals with {110}lime //{10$\bar{1}$4}calcite (oriented at an angle of

~75°) developed on the former calcite cleavage planes. Sintering does not change the oriented structure formed after calcite decomposition as deduced from pole figures of CaO planes at $T >$ 850°C. These results indicate that the calcite thermal decomposition reaction is topotactic, as has been suggested by previous XRD studies (Singh Dev, 1972). However, the orientation relationships reported in previous works are not mutually consistent, which has precluded an unambiguous description of the (possible) topotactic relationships in calcite-lime transformation.

TEM Analysis.

Calcite pseudomorphs calcined at 750°C show the strongest reflections of CaO in SAED patterns. The partially decomposed crystals were highly porous (pore size ~5-10 nm) and were made up of oriented rods (~20-50 nm long and 5 nm in thickness). CaO crystal size increased with T up to 850°C, when full decomposition occurs. The sizes of CaO nanocrystals observed with the TEM are in agreement with those determined by XRD peak broadening analysis. At $T>850$°C, the porosity of the aggregates was reduced and the average pore size increased up to ~30 nm. At 1100°C, individual micrometer-sized CaO crystals were observed. The $h00$, $0k0$ and $hk0$ reflections in SAED pattern of such crystals were broad and slightly ellipsoidal. This suggests that such large crystals are formed by a highly oriented aggregate of the nanocrystals observed at lower T. Porosity is lost and crystals attach along equally oriented faces during aggregation, thus minimizing surface energy. This is the first time that such an oriented aggregation mechanism is proposed to explain solid state crystal coarsening.

Decomposition of calcite crystals *in situ* and *in vacuo*, was observed following exposure to the electron beam in the TEM. The calcite crystal in Figure 2a (which was oriented along the $[\bar{4}41]$ zone axis) transformed into an oriented aggregate of CaO crystals, as revealed by the $[110]_{lime}$ zone-axis SAED pattern (inset in Fig. 2b). SAED patterns are consistent with the orientation relationship determined by 2D-XRD and also show that $[\bar{4}41]_{calcite}//[110]_{lime}$. Three sets of CaO nanorods oriented at ca. 120° can be observed (Fig. 2c). Although all the data point to a topotactic transformation, it should be noted that there is not a straightforward structural

similitude between $[\bar{4}41]_{calcite}$ and $[110]_{lime}$ or $(110)_{lime}$ and $(10\bar{1}4)_{calcite}$. However, if the conversion occurs by lost of CO_2 accompanied by limited atom displacement and shrinking normal to $<\bar{4}41>_{calcite}$ in $(10\bar{1}4)_{calcite}$, the parent structure readily yields the product one with $\{110\}_{lime}//\{10\bar{1}4\}_{calcite}$. Note that two sets of equivalent $<\bar{4}41>$ directions exist on $(10\bar{1}4)_{calcite}$ at and angle of 75°. This is the angle between the two sets of $(200)_{lime}$ in the 2D-XRD pole figures. This, along with TEM-SAED results, demonstrates that two families of lime crystals oriented at 75° form on each calcite cleavage plane upon solid state transformation along equivalent $<\bar{4}41>$ directions. These directions show the maximum structural similitude between reactant and $[110]_{lime}$, thus facilitating the topotactic transformation.
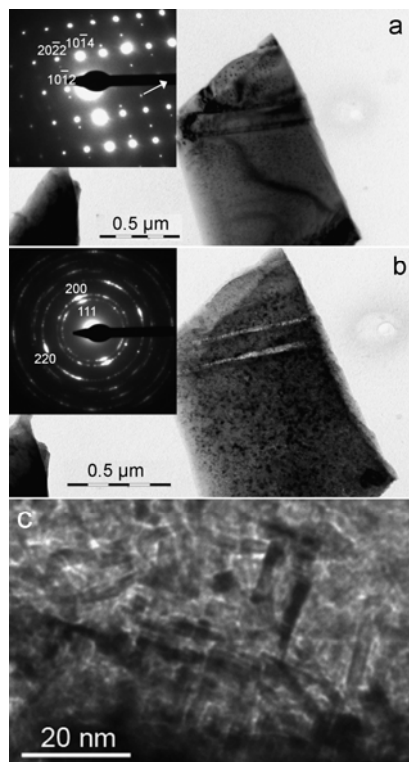
fig 2. Calcite crystal undergoing in situ decomposition in the TEM: (a) calcite crystal observed along the $[\bar{4}41]$ zone axis. The arrow in SAED pattern shows spots corresponding to a twin.; (b) the same crystals after beam damage showing discrete SAED spots (inset) corresponding to the 111, 200 and 220 reflections of CaO; (c) detail of transformed area in (b) showing oriented nanorods of CaO.

CONCLUSIONS.

2D-XRD and TEM-SAED analyses of the calcite/lime textural relationships show that the thermal decomposition of Iceland spar single crystals is pseudomorphic and topotactic, with $\{10\bar{1}4\}_{calcite}$

$//\{110\}_{CaO}$ and $<\bar{4}41>_{calcite}//<110>_{CaO}$. This reaction begins with the formation of a mesoporous structure made up of oriented rod-shaped CaO nanocrystals, which collapsed due to strain accumulation. Finally, sintering progresses up to the maximum T reached (1150°C). These mechanisms resulted in the loss of mesopores and growth of micrometer-sized pores. These results enable us to propose a novel model for the thermal decomposition of calcite that explains how decarbonation occurs at the atomic scale via a topotactic mechanism which is independent of the experimental conditions. This gained knowledge may help constrain calcinations condition to achieve best properties for industrial applications of lime as well as help to interpret textural relationships found in natural samples.

REFERENCES.

Beruto, D., Searcy, A.W., Kim, M.G. (2004): Microstructure, kinetic, structure, thermodynamic analysis for calcite decomposition: Free-surface and powder bed experiments. Thermochim. Acta **424**, 99-109.

Best, M.G. (1982): Igneous and Metamorphic Petrology. Freeman, New York.

Boynton, R.S. (1980): Chemistry and Technology of Lime and Limestone (2nd edition). Wiley-Interscience, New York.

Elert, K., Rodriguez-Navarro, C., Sebastian Pardo, E., Hansen, E., Cazalla, O. (2002): Lime mortars for the conservation of historic buildings. Studies in Conservation **47**, 62-75.

Grapes, R. (2006): Pyrometamorphism. Springer, Berlin.

Martín-Ramos, J. D. (2004): XPowder: A Software Package for Powder X-Ray Diffraction Analysis, Version 2004.03, [www.xpowder.com].

O'Keefe, J.D.& Ahrens, T.J. (1989): Impact production of CO_2 by the Cretaceous/Tertiary extinction bolide and the resultant heating of the Earth. Nature **338**, 247–249.

Rodriguez-Navarro, A.B. (2007): Registering pole figures using an X-ray single-crystal diffractometer equipped with an area detector. J. Appl. Crystallography **40**, 631-634.

Singh Dev, R. (1972): Topotaktische Phänomene bei der Calcinierung, Sulfatisierung und Chloridisierung einiger Karbonat-Einkristalle. Neues Jahrbuch für Mineralogie Monatshefte **1**, 12-22.